Verlag, Berlin, 1992).
3. A. V. Baez, *J. Opt. Soc. Am.* **42**, 756 (1952).
4. G. W. Stroke, *Appl. Phys. Lett.* **6**, 201 (1965).
5. J. T. Winthrop and C. R. Worthington, *Phys. Lett.* **15**, 124 (1965); *ibid.* **21**, 413 (1966).
6. G. L. Rogers and J. Palmer, *J. Microsc. (Oxford)* **89**, 125 (1969).
7. S. Aoki and S. Kikuta, *Jpn. J. Appl. Phys.* **13**, 1385 (1974).
8. B. Reuter and H. Mahr, *J. Phys. E* **9**, 746 (1976).
9. A. M. Kondratenko and A. N. Skrinsky, *Opt. Spectrosc. (USSR)* **42**, 189 (1977), in *Optical Information Processing*, E. S. Barrekette, G. W. Stroke, Y. E. Nesterikhin, W. E. Kock, Eds. (Plenum, New York, 1978), vol. 2, p. 1.
10. M. Howells and J. Kirz, *AIP Conf. Proc.* **118**, 85 (1984).
11. J. C. Solem and G. C. Baldwin, *Science* **218**, 229 (1982).
12. J. C. Solem, *J. Opt. Soc. Am.* **B3**, 1551 (1986).
13. ______ and G. F. Chapline, *Opt. Eng.* **23**, 193 (1984).
14. W. S. Haddad, D. Cullen, J. C. Solem, K. Boyer, C. K. Rhodes, in *OSA Proceedings on Short Wavelength Coherent Radiation: Generation and Applications*, R. W. Falcone and J. Kirz, Eds. (Optical Society of America, Washington, DC, 1988), vol. 2, p. 284.
15. In Gabor x-ray holography, a plane wave serves both to illuminate the specimen and to provide a reference wave that is collinear with it. The interference pattern between the object wave and the in-line reference wave is recorded on a high-resolution detector such as the x-ray resist polymethylmethacrylate (PMMA). X-ray Gabor holograms can be reconstructed optically (*17*) or enlarged with electron or atomic force microscopy and reconstructed numerically (*16*).
16. M. Howells *et al.*, *Science* **238**, 514 (1987), C Jacobsen, M. Howells, J. Kirz, S. Rothman, *J. Opt. Soc. Am.* **A7**, 1847 (1990).
17. D. Joyeux, S. Lowenthal, F. Polack, A. Bernstein, in *X-Ray Microscopy II*, D. Sayre, M. Howells, J. Kirz, H. Rarback, Eds. (Springer-Verlag, Berlin, 1988), p. 246, D. Joyeux and F. Polack, in *OSA Proceedings on Short Wavelength Coherent Radiation: Generation and Applications*, R. W. Falcone and J. Kirz, Eds. (Optical Society of America, Washington, DC, 1988), vol. 2, p. 295.
18. J. E. Trebes *et al.*, *Science* **238**, 517 (1987).
19. G. W. Stroke, R. Restrick, A. Funkhouser, D. Brumm, *Phys. Lett.* **18**, 274 (1965).
20. I. McNulty *et al.*, *Nucl. Instrum Methods* **A291**, 74 (1990).
21. I. McNulty, thesis, State University of New York at Stony Brook (1991).
22. H. Rarback *et al.*, *J. X-ray Sci. Technol.* **2**, 274 (1990).
23. All windows, as well as the zone plate and specimen substrates, consist of 250-µm-square, 100- to 120-nm-thick silicon nitride membranes supported by silicon frames. These membranes transmit 61 to 66% of the incident radiation at 3.4 nm.
24. E. Anderson, *SPIE Proc.* **1160**, 2 (1990).
25. The CCD (model TH7883CDA-NF) was made by Thomson Composants Militaires et Spatiaux, Courbevoie, France. The optically sensitive portion of the array is a single field of 576 by 384 pixels.
26. The high-efficiency phosphor P31 (ZnS:Cu) is commonly used in cathode ray tube displays. See R. Hertel, *Reference Data for Radio Engineers* (ITT Electro-Optics Corp., Fort Wayne, IN, 1975), pp. 17–35. We are grateful to R. Peterson for the phosphor coating.
27. S. Aoki and S. Kikuta, in *AIP Conf. Proc.* **147**, 49 (1986).
28. J. Brase, T J. Yorkey, D C. Peters, in "X-ray microimaging for the life sciences," *Lawrence Berkeley Laboratory Report LBL-27660*, D. T. Attwood and B. Barton, Eds. (Lawrence Berkeley Laboratory, Berkeley, CA, 1989), p. 74.
29. Zone plate and test object fabrication were supported by D. Attwood under U.S. Department of Energy grant DE-AC03-76SF00098. F. Camillo, C.-H. Ko, E. Kohandoust, S. Lindaas, H Rarback, S. Rock, and X. Zhang provided valuable assistance. We thank D. Sayre for helpful comments and stimulating discussion. The work was supported by the U.S. Department of Energy under grant DE-FG02-89ER60858 and carried out at the NSLS, which is supported by the U.S. Department of Energy Office of Basic Energy Sciences.

2 December 1991; accepted 16 March 1992

Order and Low Dimensionality in the Organic Superconductor (BEDT-TTF)$_2$Cu(NCS)$_2$ Revealed by STM

R. Fainchtein,* S. T. D'Arcangelis, S. S. Yang, D. O. Cowan

Single-crystal samples of [(BEDT-TTF)$_2$]$^+$[Cu(NCS)$_2$]$^-$ were synthesized and studied with a scanning tunneling microscope (STM). Real-space images of the anion and cation surfaces with molecular resolution were obtained. The images show no evidence of structural disorder or stacking faults previously suggested. The presence of an additional modulation commensurate with the lattice provides evidence of a lattice distortion. The cause of this modulation is unknown. The presence of a charge density wave in the material would have implications on the dimensionality of the material that may explain the peculiar temperature dependence of the electrical conductivity. This interpretation is consistent with the calculated Fermi surface, which allows nesting of the wave vector.

The recent progress in the race to increase the superconducting transition temperature (T_c) in organic materials has been motivated by the discovery of the superconducting properties of the κ-phase (BEDT-TTF) (or ET) compounds. Since the synthesis in 1990 (*1*) of κ-phase di[bis(ethylenedithiolo)tetrathiafulvalene] copper(I)bis(isothiocyanate), κ-$[(ET)_2]^+[Cu(NCS)_2]^-$, which exhibits a T_c = 10.4 K in dc resistance measurements, a new series of κ-phase compounds has been synthesized with T_c values in excess of 11 K (*2*).

The x-ray studies of κ-$[(ET)_2]^+$-$[Cu(NCS)_2]^-$ (*1, 3*) have revealed a structure formed by the interstacking of planes of standing ET molecules that form dimers in a two-dimensional (2-D) network arrangement, together with planes formed by $[Cu(NCS)_2]$ polymer chains located between the ET planes (see Fig. 1). These structural studies have opened up discussions on the role and position of the $[Cu(NCS)_2]$ counteranions within the plane. The presence of positional disorder and a stacking fault in the direction of the *b* axis every four unit cells have been proposed (*4*). These structural models together with the idea of a diminished role in the electrical conductivity played by the anions (as insulating spacers between the ET conduction planes) have been used to explain the behavior of these κ-phase materials.

The electrical transport properties of the κ-phase ET compounds display a peculiar temperature behavior that is not yet fully understood. The temperature dependence of the electrical resistivity of the material reveals the existence of three regimes: (i) a metallic regime (decrease of resistance with temperature) from room temperature to 240 K; (ii) an activated or "semiconducting" regime (increase of resistance with temperature) from 240 to 90 K; and (iii) another metallic regime from 90 to 10.8 K before the compound finally makes the transition to a superconductor with a mid-range T_c of 10.4 K (*5*).

In this study a scanning tunneling microscope (STM) was used in an effort to resolve the structural uncertainties and provide insight into the role of the anions in the conductivity of the material. The results may also suggest a possible explanation for the peculiar temperature dependence of the electrical resistivity in this material.

Samples of κ-$[(ET)_2]^+[Cu(NCS)_2]^-$ were prepared by standard electrochemical methods (*5*). Four-probe dc resistance measurements were made on single crystals from room temperature to liquid helium temperature.

STM images of κ-$[(ET)_2]^+[Cu(NCS)_2]^-$ were taken in air at room temperature. The measurements were made with a commercial STM (*6*) operated under either standard constant-current or constant-height conditions (*7*). No apparent differences in the images were observed in the two modes of operation. The crystals were mounted on Au films and fixed to the substrates with conductive Ag paint. The tunneling current (i_{tun}) was set to values of 1 nA. Scans

---

R Fainchtein, Applied Physics Laboratory, Johns Hopkins University, Laurel, MD 20723.
S. T. D'Arcangelis, S. S. Yang, D. O. Cowan, Chemistry Department, Johns Hopkins University, Baltimore, MD 21218.

---

*To whom correspondence should be addressed.

were made with positive and negative tip bias voltages (V_{tip}) within ±200 mV. No apparent differences were observed as a consequence of changes in the tip bias within the specified range. Tunneling resistances were kept at or above 10^7 ohms. The images were not manipulated except for a background plane subtraction. We used Pt tips with 20% Ir (8). The top flat phase of the flake-shaped crystals was imaged in all cases. STM scans ranged in size from 30 by 30 Å to 700 by 700 Å. Images of the surface of two different crystals are presented.

Figure 2A is a 67 by 67 Å STM image of the *bc* plane. The superimposed drawing in Fig. 2B corresponds to the unit cell and the structure of the rings that form the upper extremes of the ET cations closer to the anion plane. Because the tunneling current is extremely distance-dependent, only the atoms close to the surface make a significant contribution to the image; therefore, only the extreme rings of the ET molecule will be observed in this plane (9). The model was first scaled to the dimensions of the image and then translated and rotated to find the best match; the shape and distances of and within the unit cell were preserved. The unit cell is repeated 3 × 3 times, and the agreement with the image is excellent. The image was taken in a constant-height mode, which means that the bright intensity spots correspond to locations of high tunneling current. The resolution obtained is only good to show the position of the ET molecules within the surface.

Figure 3A is a 70 by 70 Å STM image of the *bc* plane. The superimposed drawing in Fig. 3B corresponds to the structure of the anions as determined by x-ray diffraction (3), scaled and rotated to find the best match. The unit cell is once again repeated 3 × 3 times, and the agreement with the image is excellent. Long-range distortions may be due to thermal drift between the STM and the sample, caused by differences in thermal expansion. The center of the Y-shaped repeated structure corresponds to the position of the Cu atom connected on one end to the S atom of the preceding unit and to two NCS atom sequences at the Y branches. An important feature is the difference in intensities of adjacent Cu–S bonds in the STM image. This difference in intensities identifies, within the resolution provided by the images, an additional modulation commensurate with the lattice with *b* and *c* periods. Because this image was taken in a constant-current mode, the bright intensity spots correspond to positions where the tip had to pull away from the surface to maintain a constant current.

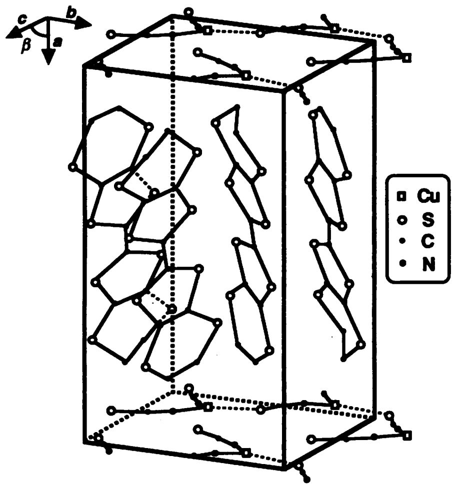

Fig. 1. The crystal structure of κ-[(BEDT-TTF)$_2$]$^+$[Cu(NCS)$_2$]$^-$.

Larger STM scans of the same samples revealed regular structures like the ones shown and showed no evidence of positional disorder. The images presented reveal the structure of the cations and anions. The imaging of the cations or anions is not junction bias–dependent for tip voltages within the range described; it is sample-dependent (these images were taken on two different crystals). The resulting STM image is determined by the way the particular crystal terminates and not by the tunneling conditions (tunneling current or bias voltage settings) or the different modes of operating the STM (constant current or constant height). This means that images that reveal the cation structure were taken on a crystal in which the ET molecules formed the last layer, and similarly images that reveal the anion structure were taken on a crystal in which the Cu(NCS)$_2$ polymeric chains formed the last layer. Both crystals were synthesized in the same batch. This implies that the appearance of one or the other element in the image is related to the way the crystal terminates.

Of particular importance in this study are the high-resolution images of the anions (Fig. 3). The STM images provide direct evidence of the lack of disorder and structural irregularities proposed by other studies (*1*, *4*, *10*). Because the STM is a surface probe of the local electron density of states

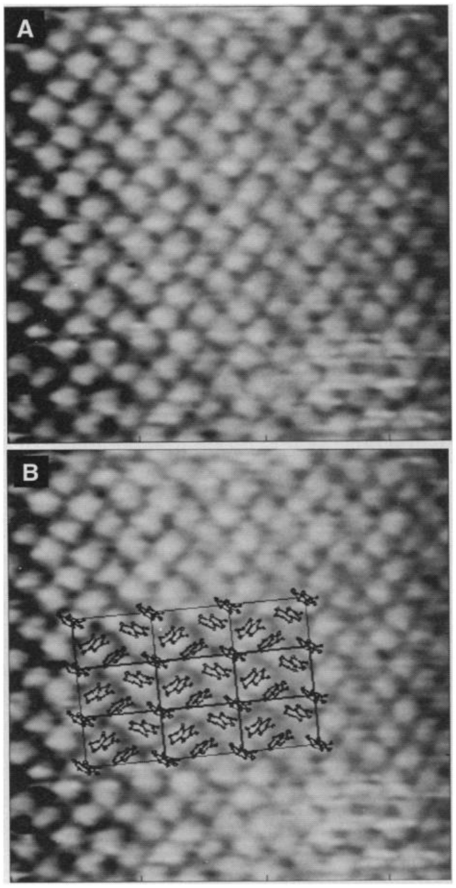

Fig. 2. (**A**) STM image of a 67 by 67 Å scan of the *bc* plane of the crystal κ-[(BEDT-TTF)$_2$]$^+$[Cu(NCS)$_2$]$^-$. (**B**) STM image with the molecular structure of the outer ring of the ET cations (*9*) projected onto the *bc* plane superimposed (V_{tip} = −200 mV, i_{tun} = 1 nA, constant-height mode).

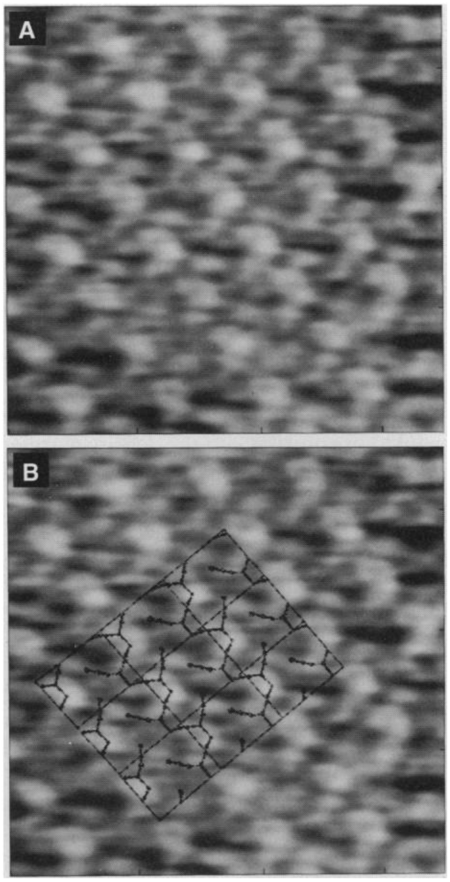

Fig. 3. (**A**) STM image of a 70 by 70 Å scan of the *bc* plane of the crystal κ-[(BEDT-TTF)$_2$]$^+$[Cu(NCS)$_2$]$^-$. (**B**) STM image with the projection of the molecular structure of the anions superimposed (V_{tip} = 50 mV, i_{tun} = 1 nA, constant-current mode).

near the Fermi level (*11*), the bright spots located above the Cu–S bonds in the anion images (Fig. 3) provide direct evidence of an additional modulation in the spatial dependence of the electron density of states. What makes this result surprising is the fact that, although the environment of both Cu atoms that appear within the unit cell is the same (equivalent positions), only one of these S–Cu bonds appears highlighted in the STM images. The presence of an additional modulation in the STM images is indicative of a fluctuation in the atomic arrangement of the unit cell. The nature of this modulation is unknown. Other experimental results that may suggest a possible interpretation are examined below.

Analysis (*12*) of the Shubnikov–de Hass effect on κ-[ET]$^+$[Cu(NCS)$_2$]$^-$ (*13*) suggests that the anisotropy of the in-plane conductivity implies the existence of nested states in the Fermi surface and the presence of a charge density wave (CDW). The strongest manifestation of such structural anisotropy in the *bc* plane would come from the anions because the [(ET)$_2$] dimers arrange perpendicular to one another to form a 2-D network, and therefore an anisotropy in this plane would come from small structural deviations of the 2-D pattern. The polymeric chains formed by the anions, on the other hand, provide a natural 1-D character to the structure and could indeed be responsible for the anisotropy of the electrical conductivity in the *bc* plane. This would give the anions a more important role in the normal conductivity of the material than previously thought. X-ray absorption fine structure results have corroborated this conclusion (*14*), which may be manifested in the fact that the anions are so well resolved in the STM images. If the anions were simply insulating spacers between the ET conduction planes, they would not contribute to the density of states near the Fermi level and the images would be the result of fluctuations in the tunneling barrier height. Because the anion images reflect height corrugations on the order of 1 Å, this would imply barrier height fluctuations of $\sim$1 eV or more (depending on the tip to sample distance) over the [Cu(NCS)$_2$] atomic distances (*15*).

The existence of a CDW in the material would not be consistent with a modulation that has the same period as the undistorted lattice. We speculate that, if the additional modulation present in the anion images was due to the presence of a CDW commensurate with the lattice as observed in other low-dimensional organic systems (*16*), there should be an additional modulation (with longer period) that the current study does not resolve.

The presence of a CDW in the material with an incommensurate to commensurate transition at 240 K would explain the opening of a gap in the electron density of states near the Fermi level and the transition in the resistance versus temperature to a temperature-activated regime. As the temperature is decreased, the material is known to experience a pronounced contraction in the *c* direction and an expansion in the *a* direction (*3, 17*). The contraction in the *c* direction would bring the polymeric chains closer together, increasing their interaction and diminishing the 1-D character of the material. These circumstances may cause the projection of the Fermi surface along the *bc* plane to become more circular, the nested states and the CDW to disappear, the gap to close, and the material to become metallic. This model would be consistent with the reported suppression of the anomalous temperature versus resistance behavior by the application of pressure (*18*) and the enhancement of this behavior by the application of tension along the *b* direction (*19*). Low-temperature STM studies are needed to test this hypothesis.

REFERENCES AND NOTES

1. H. Urayama *et al*, *Chem Lett* **1988**, 55 (1988).
2. J M Williams *et al.*, *Science* **252**, 1501 (1991).
3. H Urayama *et al*, *Chem Lett.* **1988**, 463 (1988)
4. S. Ravy, J. P. Pouget, C Lenoir, P Batail, *Solid State Commun* **73**, 37 (1990) The presence of a stacking fault has been found to be sample-dependent J. P Pouget, discussion following presentation of the paper listed in (*5*).
5. R Fainchtein, S T D'Arcangelis, S S Yang, D. O. Cowan, in *Proceedings of the Fall Meeting of the Materials Research Society, Symposium on Electrical Optical and Magnetic Properties of Organic Solid State Materials*, Boston, MA, 2 to 6 December 1991 (Materials Research Society, Pittsburgh, in press)
6. Nanoscope II from Digital Instruments, Santa Barbara, CA
7. R Fainchtein and J C Murphy, *J Vac. Sci Technol B* **9**, 1013 (1991)
8. R Fainchtein and P R Zarriello, *Ultramicroscopy*, in press
9. M Yoshimura *et al.*, *Phys Rev B* **43**, 13590 (1991)
10. K Oshima *et al*, *Synth Metals* **41–43**, 2175 (1991)
11. J Tersoff and D R. Hamann, *Phys Rev. Lett* **50**, 25 (1983). *Phys Rev B* **31**, 2 (1985).
12. S A Wolf and V Z. Kresin, in *Organic Superconductivity*, V Z Kresin and W A Little, Eds. (Plenum, New York, 1990), p. 31
13. K Oshima *et al*, *Phys Rev B* **38**, 938 (1988)
14. T Doi *et al*, *J Phys Soc Jpn* **60**, 1441 (1991)
15. R Wiesendanger *et al*, *Surface Sci* **189/190**, 24 (1987), N D Lang, *Phys Rev B* **37**, 10395 (1988)
16. S Ravy, J P Pouget, L. Valade, J P Legros, *Europhys Lett* **9**, 391 (1989), R Comes *et al*, *Phys Rev Lett* **35**, 1518 (1975)
17. Y Watanabe, T Sasaki, H Sato, N Toyota, *J Phys. Soc Jpn* **60**, 2118 (1991)
18. I D Parker *et al*, *J Phys Condens. Matter* **1**, 4479 (1989) N Toyota and T Sasaki, *Solid State Commun* **74**, 361 (1990)
19. H Kusuhara *et al*, *Solid State Commun* **74**, 251 (1990)

20. Work supported in part by the U.S Department of the Navy under contract N00039-89-C-0001 and in part by the National Science Foundation under grant DMR-8921071

23 December 1991, accepted 24 March 1992

Interaction Cloning: Identification of a Helix-Loop-Helix Zipper Protein That Interacts with c-Fos

Michael A. Blanar and William J. Rutter

A facile method for isolating genes that encode interacting proteins has been developed with a polypeptide probe that contains an amino-terminal extension with recognition sites for a monoclonal antibody, a specific endopeptidase, and a site-specific protein kinase. This probe, containing the basic region–leucine zipper dimerization motif of c-Fos, was used to screen a complementary DNA library. A complementary DNA that encoded a member of the basic-helix-loop-helix–zipper (bHLH-Zip) family of proteins was isolated. The complementary DNA–encoded polypeptide FIP (Fos interacting protein) bound to oligonucleotide probes that contained DNA binding motifs for other HLH proteins. When cotransfected with c-Fos, FIP stimulated transcription of an AP-1–responsive promoter.

Many cellular processes involve specific protein interactions. Identification of the interacting proteins can be a prodigious task if one uses conventional biochemical approaches. We have developed a convenient method, involving molecular cloning, that facilitates the detection and isolation of the interacting entity. This method has been used to study the interactions of transcription factors.

The leucine zipper (Zip) and the helix-loop-helix (HLH) dimerization motifs are found in eukaryotic transcription factors that are members of the basic region–Zip (bZip) and bHLH families, respectively. The Zip and HLH domains permit the formation of homodimers or heterodimeric combinations among family members. The Zip domain is characterized by a heptad repeat of leucine residues that form an amphipathic α-helical structure (*1*). When

---

Hormone Research Institute and Department of Biochemistry and Biophysics, University of California at San Francisco, San Francisco, CA 94143